Pile-soil interaction and settlement effects induced by deep excavations

Korff, M.; Mair, R; van Tol, AF

DOI
10.1061/(ASCE)GT.1943-5606.0001434

Publication date
2016

Document Version
Final published version

Published in
Journal of Geotechnical and Geoenvironmental Engineering

Pile-Soil Interaction and Settlement Effects Induced by Deep Excavations

Mandy Korff, Ph.D.[1]; Robert J. Mair[2]; and Frits A. F. Van Tol[3]

Abstract: Deep excavations may cause settlement and damage to adjacent buildings, even if they are found on piles. The corresponding pile deformations are determined by axial and lateral effects. This paper describes an analytical model relating axial pile deformation to the vertical soil displacement resulting from the deep excavation and also suggests ways to determine the pile response to lateral displacements. The axial pile-soil interaction is clearly different for end-bearing and friction piles. Common generalizations that end-bearing piles settle the same as the soil settlement at the base level and friction piles with the ground surface settlement present lower and upper bounds, which are only valid for certain idealized cases. The settlement of piles with a large component of shaft friction is determined mainly by the actual load on the pile relative to the pile ultimate capacity. The lateral pile response is governed mainly by the relative stiffness of the pile to the soil. The proposed model was validated with measurements of the North South Line project in Amsterdam. **DOI: 10.1061/(ASCE)GT.1943-5606.0001434.**

Author keywords: Pile settlement; Pile lateral loads; Skin friction; Soil-pile interactions; Excavation; Soil deformation; Settlement; Nonlinear analysis.

Introduction

Underground construction supports the quality of life in cities by improving the availability and quality of the space above ground. Tunnels and deep excavations can, however, not be realized without affecting adjacent structures. An assessment of the potential building damage during construction should ideally consist of the following steps: (1) determine greenfield displacements; (2) impose displacements onto building; (3) assess potential damage; and (4) design protective measures if necessary. Most methods to assess the impact on the buildings have originally been developed for tunneling projects and buildings with shallow foundation and can be improved by specifically looking at piled buildings near deep excavations. This paper provides a method to evaluate the axial response of piled buildings to the construction of deep excavations in soft soil conditions and also gives guidance to include the lateral pile response.

Pile-Soil Interaction Methods

The response of piles to excavation-induced soil deformations resembles the response of piles to other soil deformations such as those caused by tunneling or groundwater lowering. Specifically for piles subjected to tunneling, field tests by Kaalberg et al. (2005) and centrifuge tests by Bezuijen and van der Schrier (1994) and Jacobsz et al. (2005) showed that deformation of piles caused by tunneling can mostly be explained by settlement of the soil layer around the pile base and, to a much lesser extent, by stress relief. Jacobsz et al. (2005) showed, on the basis of three case studies in the Channel Tunnel Rail Link project, a difference between end-bearing and friction piles. End-bearing piles follow the greenfield settlement at the pile base for small volume losses. Friction piles alter the greenfield subsurface displacements and follow more or less the surface settlements as a conservative approach. Models to determine the influence of tunneling on a single pile or a pile group are given by Chen et al. (1999) and Xu and Poulos (2001).

Bending moments in especially long piles adjacent to tunnels can be significant, as shown by Loganathan et al. (2001) and Ong et al. (2007). Centrifuge tests, such as the ones by Leung et al. (2000, 2003), Goh et al. (2003), and Ong et al. (2006, 2009) proved for long piles (Fig. 1) these bending moments to be very important. For short piles and very stiff, multistrutted, deep excavations (two to three times deeper than the piles), settlements are likely to be much more important than horizontal deflections.

Axial soil displacements cause changes in the positive and negative shaft friction along the pile, depending on the pile and soil stiffness, the working load on the pile, and the soil displacements. Methods to determine the axial response of piles near deep excavations have been described most extensively by Poulos and Chen (1997) and Zhang et al. (2011). Zhang et al. (2011) concluded that the working load initially present on the pile before the excavation takes place is an important factor to take into account. An increasing working load indicates an increasing pile deformation related to the excavation and a decreasing additional axial force to be developed. Ultimately, for a pile in failure, no additional axial force can be mobilized. The work of Zhang et al. (2011) also includes the lateral effect on the piles, based on work by Goh et al. (1997) for piles loaded by embankment deformations.

Axial and the lateral loading of the pile are actually not independent in case of excavations. For pile groups, the settlement

[1]Senior Specialist, Deltares, P.O. Box 177, NL-2600 MH Delft, Netherlands (corresponding author). E-mail: mandy.korff@deltares.nl

[2]Professor, Head of Civil Engineering Division, Cambridge Univ., Trumpington St., Cambridge CB2 1PZ, U.K. E-mail: rjm50@eng.cam.ac.uk

[3]Professor of Foundation Engineering, Delft Univ. of Technology, Netherlands and Member of Scientific Board Deltares, P.O. Box 177, NL-2600 MH, Delft, Netherlands. E-mail: frits.vantol@deltares.nl

Note. This manuscript was submitted on September 5, 2014; approved on September 16, 2015; published online on April 11, 2016. Discussion period open until September 11, 2016; separate discussions must be submitted for individual papers. This paper is part of the ***Journal of Geotechnical and Geoenvironmental Engineering***, © ASCE, ISSN 1090-0241.

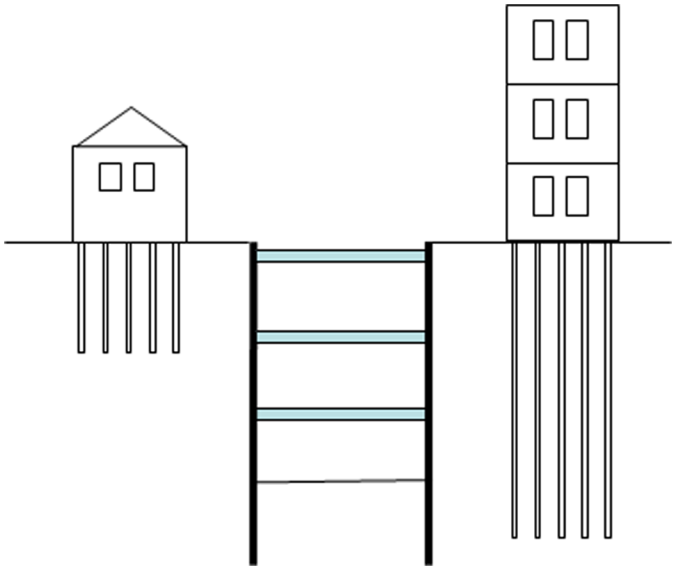

Fig. 1. Deep excavation with short piles and long piles; short pile deformations are mainly governed by settlement, and long piles, by deflection

of the piles can be reduced if the horizontal soil deformation is reduced by the bending stiffness of the piles. This effect can be simulated for example in FEM calculations but is not taken into account in this paper as is the case for the uncoupled approaches commonly used.

For deep excavations with relatively short piles in soft soils and a pre-existing condition of negative skin friction, a method is described in this paper to deal with subsequent loading stages. Furthermore, this study is intended to show the relative importance of the relevant parameters, to raise awareness of the differences in pile response to excavations depending on the initial loading conditions and friction piles versus end-bearing piles. The method can be used to determine the axial response of piles related to excavations in simplified conditions, whereas a spring model is given for more complicated conditions such as end-bearing piles or piles with varying shaft friction with depth and for lateral loading. Dimensionless graphs are provided to enable insight into the factors governing the axial soil-pile interaction.

Axial Pile Response

The axial deformation of the pile head, p, is determined by the following effects:

- Settlement caused by the reduction of pile capacity by lower stress levels (p_s);
- Settlement caused by soil displacement below the base of the pile (p_b);
- Settlement related to the development of negative (and/or positive) skin friction by relative movements of the soil and the pile shaft (p_i); and
- Additional pile settlement caused by redistribution of pile load over the piles under the building slab, building wall, foundation cap, or beam (p_r).

For end-bearing piles, p_s is expected to be significant only if the pile bases are very close to the excavation, as shown similarly for tunnels by Kaalberg et al. (2005) and Lee and Ng (2005). Stress relief around the pile base can lead to additional mobilization of positive shaft friction. The settlement under the pile base, p_b, may be calculated without interaction with the piles, for example, with a finite-element (FE) analysis or by using the Aye et al. (2006) method for deeper soil displacements caused by excavations. The interaction component, p_i, is different for friction piles and end-bearing piles. If the soil displaces an equal amount over the whole length of the pile, the pile settles with this amount of soil settlement. Any other shape of soil settlement (either larger at the top as expected for excavations or larger near the pile base as expected for tunneling) will cause additional negative and positive shaft friction. For a piled building with certain stiffness, redistribution of loads takes place. If this happens, the external load on the pile changes, leading to a new equilibrium. This effect, p_r, should be determined by a coupled analysis for a pile group, such as with a boundary element method as described by Xu and Poulos (2001) or with the D-Pile Group model with a cap over the piles as described in Bijnagte and Luger (2000).

For many cases, the effect of stress relief p_S can be assumed small. The effect of load redistribution p_r or settlement below the base p_b can be determined on the basis of the methods previously described. The interaction effect p_i depends largely on existing conditions and is studied in this paper in more detail.

Mobilization of Skin Friction

The interaction effect p_i along the pile caused by excavation-induced settlements is similar to the concept of negative skin friction development. Negative skin friction can be determined by a total stress approach (α-method), an effective stress approach (β-method) or empirically from in situ test results such as cone penetration test (CPT). The neutral level is commonly described as the level at which the interface shear stress changes from negative to positive. The maximum force in the pile is found at this level. For single piles, the negative skin friction is primarily controlled by the free-field subsoil settlement profile and the mobilization of the pile shaft resistance. If ground settlements along the pile occur, negative skin friction will develop. This will lead to three possible situations, shown in Fig. 2:

- In case of friction piles, negative and positive friction will both develop along the pile to obtain a new equilibrium. The pile will settle a certain amount between the minimum and maximum soil displacement found along the pile.
- For end-bearing piles, the additional negative shaft friction is balanced by additional base resistance. If base capacity is sufficient, the pile settlement (p) will be limited to the ground settlement at the tip (p_b) plus the deformation required to mobilize the additional base capacity (p_i).
- For piles that combine friction and end bearing, the pile settlement (p) will largely depend on the neutral level and the ground settlement at that level. Such piles are encountered if base capacity is not sufficient to take the full negative friction, and additional positive friction will develop along the shaft to maintain equilibrium. This is, for example, the case for many old timber piles in historic delta cities like Amsterdam.

In the following section, the general model will be explained first, after which specific situations are given in subsequent paragraphs.

Interaction Model for Negative and Positive Friction

In this section, the effect of positive and negative shaft friction is discussed on the basis of a nonlinear analytical spring model that was developed to study the difference in behavior between friction piles and end-bearing piles (p_i, based on axial interaction for single piles). The effect of the initial loading condition of the piles is shown for pile loads varying from 0 to 100% of the maximum

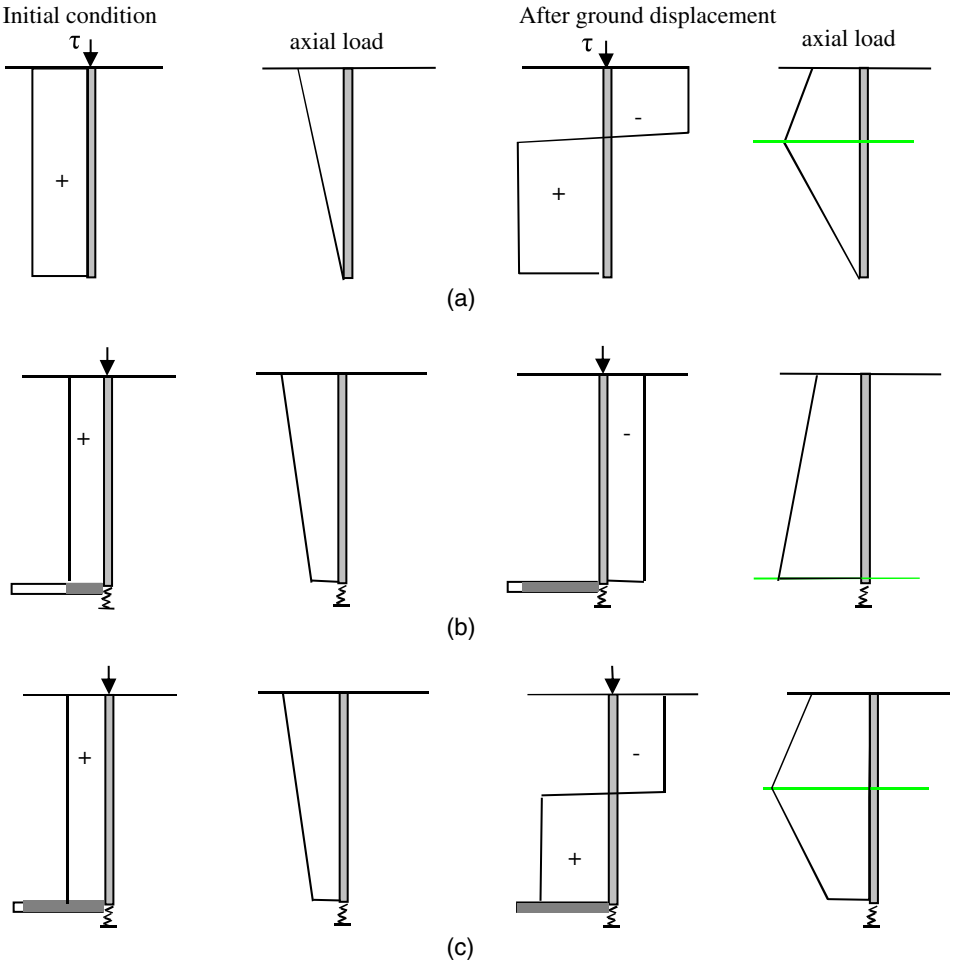

Fig. 2. Pile-ground interaction for (a) friction piles with uniform shaft friction with depth; (b) end-bearing piles; (c) combined friction and end-bearing piles; ground displacement is assumed largest at the top of the pile; neutral level is shown in green

bearing capacity Q_{max}. The pile deformation can be determined relative to the greenfield settlement of the soil by finding the depth z at which the pile deformation equals the soil settlement. This depth z, relative to the length of the pile L (z/L), is in this paper called the *interaction level*. This is close to but not the same as the *neutral level*, which is defined as the depth at which the shaft friction changes from negative to positive (Fig. 2). The *greenfield settlement* is defined as the settlement at the location of the pile as if no pile or building were present. All soil displacements referred to in this paper are greenfield values.

The deformation of the pile (p_i) related to the displacement of the soil (S_z) can be determined from the basic pile equilibrium equation

$$W = \int_0^{L_p} \tau \cdot \pi \cdot D dz + A \cdot q_b \tag{1}$$

where τ = shaft friction along the pile with diameter D; z = vertical axis (positive down along the pile); and q_b = average foundation pressure around the base in $(\mathrm{kN/m^2})$ with cross section $A(\mathrm{m^2})$. The pile is positioned from $z = 0$ to $z = L_p$, with L_p as the length of the pile (Fig. 3). The actual working load W on the pile is assumed constant (no redistribution between piles). The shaft friction τ_z is the function of the relative displacement between soil and pile and the relative displacement D_z, at which τ_{max}, the maximum shaft friction, is reached in a bilinear approach (Fig. 4). This function can be derived either from field tests or existing codes.

For friction piles, the base resistance plays only a very minor role and is neglected in this paper. Working toward a dimensionless

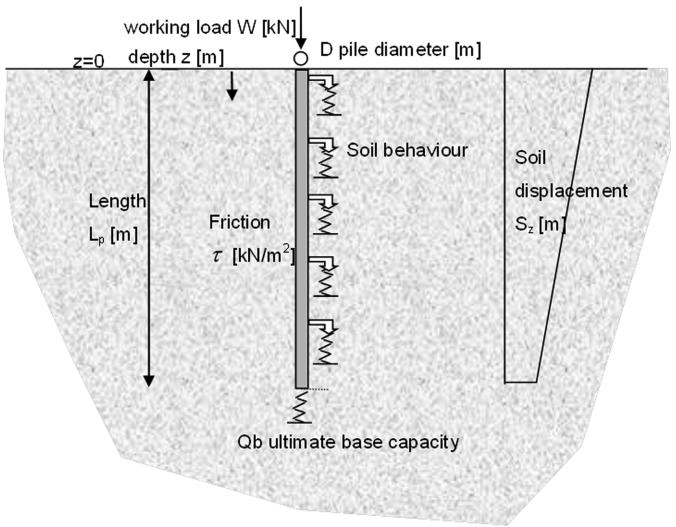

Fig. 3. Model schematization and parameters

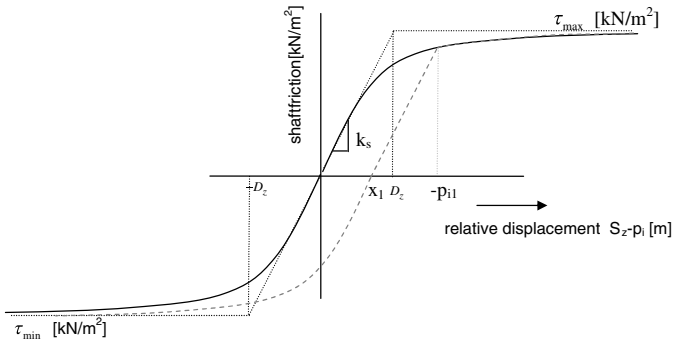

Fig. 4. Shaft friction versus relative displacement between pile and soil

representation, all variables are transformed by relating them to a characteristic dimension and are further denoted by

$$z' = z/L_p; \qquad \tau' = \tau/\tau_{av;\max}; \quad \text{and} \quad \tau'_{\max} = \tau_{\max}/\tau_{av;\max}$$

where $\tau_{av;\max}$ = average shaft friction over the pile length.

Other dimensionless variables used are

$$S'_z = S_z/D_z; \qquad p'_i = p_i/D_z; \qquad D'_z = D_z/D_z = 1$$

Eq. (1) transforms for friction piles in dimensionless form to

$$\frac{W}{Q_{\max}} = \int_0^1 \tau' dz' \tag{2}$$

The general shaft friction formula (Fig. 4)

$$\tau = \tanh\left(\frac{S_z - p_i}{D_z}\right) \cdot \tau_{\max} \tag{3}$$

becomes in dimensionless form

$$\tau' = \tanh(S'_z - p'_i) \cdot \tau'_{\max} \tag{4}$$

The initial stiffness k_s is the gradient of shaft friction τ at

$$(S_z - p_i) = 0$$

$$k_s = \frac{\tau_{\max}}{D_z} \tag{5}$$

During the initial loading of the pile (called Step 1), the shaft friction along the length of the pile can be found by solving Eq. (2) in combination with Eq. (4). The pile deformation p_{i1} will be found as a result, with the corresponding τ_1, when the initial soil displacement $S_z = 0$.

The next step is the occurrence of an external soil displacement initiated by the excavation (called Step 2). For Step 2, the formula of the shaft friction is given in three parts, represented by the striped line in Fig. 4. The unloading-reloading stiffness is the same as the initial stiffness k_s, and the original tangent hyperbolic function applies for positive and negative loading.

The dimensionless pile deformation after this step (p'_{i2}) can be found from Eq. (6)

$$\begin{aligned}
&\text{if } (S' - p'_{i2}) > -p'_{i1} \\
&\tau' = \tanh(S'_z - p'_i) \cdot \tau'_{\max} \\
&\text{if } x_1 < (S' - p'_{i2}) < -p'_{i1} \\
&\tau' = k'_s \cdot (S'_z - p'_i - x'_1) \\
&\quad \text{with } x'_1 = -\frac{\tau'_1}{k'_s} - p'_{i1} \quad \text{with } x'_1 \geq 0 \quad \text{and} \quad k'_s = 1 \\
&\text{if } (S' - p'_{i2}) < x'_1 \\
&\tau' = \tanh(S'_z - p'_i - x'_1) \cdot \tau'_{\max}
\end{aligned} \tag{6}$$

The solution of the pile deformation for Step 2 depends on the shape of the soil displacement and the shaft friction with depth, which are described in the following two sections. The pile deformation caused by the greenfield soil displacement can be found by subtracting the pile deformation from Steps 1 and 2.

The shape of the soil displacement with depth along the pile is an important parameter for the interaction between pile and soil. The settlement can be derived from monitoring data, or if monitoring data are not available, settlements can be assessed by either FE analysis or by simplified charts, such as presented by Clough and O'Rourke (1990) or Aye et al. (2006). For excavations, the settlement at the surface is usually larger than at the pile base. For this analytical model, at first a linear shape of the soil displacement is assumed

$$S'_{L_p} = S'_0 + \frac{\Delta S}{D_z} \cdot z' \tag{7}$$

where $S'_0 = S_0/D_z$, the dimensionless factor of the soil displacement at $z = 0$; $S'_{lp} = S_{lp}/D_z$, the dimensionless factor of the soil displacement at $z = L_p$; $\Delta S = S_{L_p} - S_0$.

S'_0 may be taken out of the equation, because any overall settlement of the soil along the pile can be added to the pile settlement after the interaction calculation. A different interaction settlement p_i will be found for the same surface settlement and settlement of the foundation layer, when the *shape* of the settlement with depth is not linear, for example, because of the nature of the settlement origin, such as dewatering, tunneling, or excavation. Because of the p_i settlement, a small amount of extra shaft resistance could be obtained for the extra embedment in the bearing layer. When the cone resistance in the bearing layer is not constant, also the tip resistance might be affected. Both these effects are considered to be second order and should be neglected in normal conditions.

Analytical Solution for Constant Maximum Shaft Capacity

In the simplest case, the maximum shaft friction $\tau_{\max}$ is a constant value with depth along the pile. Inserting Eq. (6) in Eq. (2) results in

$$\frac{W}{Q_{\max}} = \int_0^1 \tanh(S' - p'_i) \cdot 1 dz' \tag{8}$$

Step 1: The initial condition with $S_{z1} = 0$ becomes

$$\frac{W}{Q_{\max}} = \int_0^1 \tanh(-p'_{i1}) dz' = \tanh(-p'_1) \tag{9}$$

Eq. (9) can be solved into

$$p_{i1} = -\frac{1}{2} D_z \ln\left(\frac{1+\frac{W}{Q_{\max}}}{1-\frac{W}{Q_{\max}}}\right) \tag{10}$$

Step 2: The soil settlement takes place.

The normalized pile deformation p'_{i2} can be found by solving the following set of equations:

$$\frac{W}{Q_{\max}} = \int_0^1 \tau' dz' \tag{11}$$

with

$$\text{if } (S' - p'_{i2}) > -p'_{i1} \qquad \tau' = \tanh\left(\frac{\Delta S}{D_z} \cdot z' - p'_{i2}\right)$$

$$\text{if } x_1 < (S' - p'_{i2}) < -p'_{i1} \qquad \tau' = \frac{\Delta S}{D_z} \cdot z' - p'_{i2} - x'_1$$

$$\text{with } x'_1 = -\tau'_1 - p'_{i1} \quad \text{with } x'_1 \geq 0$$

$$\text{if } (S' - p'_{i2}) < x'_i \qquad \tau' = \tanh\left(\frac{\Delta S}{D_z} \cdot z' - p'_{i2} - x'_1\right)$$

To obtain the pile deformation caused by the soil displacement, p_{i2} is found by transforming back to dimensions: $p_{i2} = p'_{i2} \cdot D_z$. The pile settlement p_i becomes $p_i = S_0 + p_{i2} - p_{i1}$ when the overall pile settlement S_0 is reintroduced. The interaction level z_p/L_p at which p_i is equal to S_{z2} can be found for the linear soil displacement

$$\frac{z_p}{L_p} = \frac{p_{i2} - p_{i1}}{\Delta S} \tag{12}$$

Fig. 5 shows the interaction level z_p/L_p at which the pile deformation caused by the excavation is equal to the soil displacement S_{z2}. It is concluded that friction piles settle with at least the average soil displacement along the pile (for very small loads on the pile) and at most the maximum soil displacement (for piles with very high initial loads). For excavations, where the maximum soil displacement is found at the surface, the interaction level z_p/L_p decreases from halfway the pile depth to the surface (0.5–0).

In this simplest case, the pile is considered infinitely stiff, the maximum shaft friction is constant with depth, no base capacity is assumed, and the pile diameter is constant with depth. The soil displacement is a linear function of the depth along the pile. Fig. 6 shows the additional negative and positive shaft friction for such a pile for an initial load of 50% of the maximum bearing capacity.

From the head of the pile to the level called "interaction level z/L'' in Fig. 6, the soil settles more than the pile. The additional positive friction developed at larger depth balances the additional negative shaft friction in the upper section. The additional pile deformation compared to the soil displacement depends on the initial load on the pile. The neutral level after the soil displacement has taken place is close to but not the same as the interaction level. Also, the neutral level changed from its initial level at the top of the pile to the level indicated after Step 2.

The difference between the neutral level and the interaction level increases if the shaft friction along the pile is partially mobilized in the transition zone between maximum positive and maximum

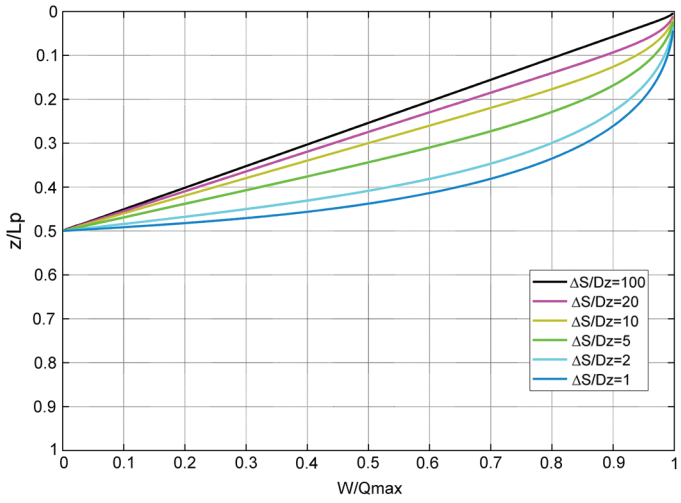

Fig. 5. (Color) Relationship between z_p/L_p and $W/Q_{\max}$ for different values of $\Delta S/D_z$ for a friction pile with infinite stiffness and constant maximum shaft friction with depth; positive values of $\Delta S/D_z$ are linked to linearly decreasing soil displacement with depth

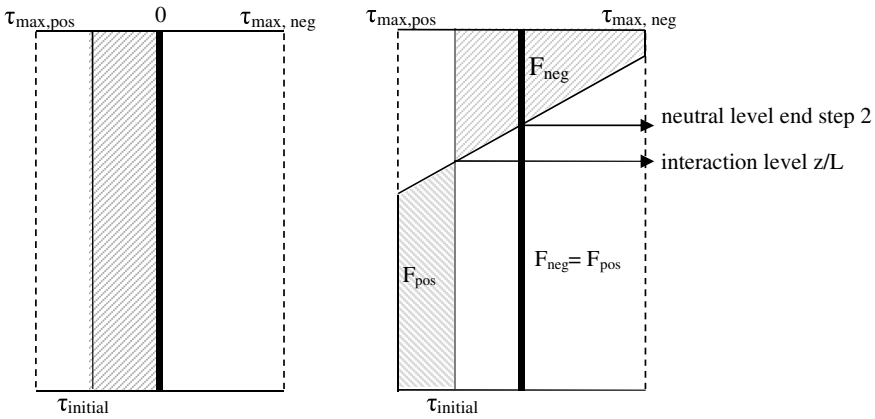

Fig. 6. Example of development of positive and negative shaft friction caused by an excavation (Step 2, on the right) after initial loading in step (Step 1, on the left)

J. Geotech. Geoenviron. Eng., 2016, 142(8): 04016034

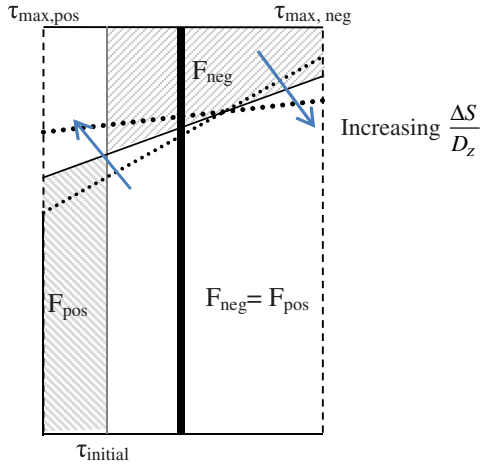

Fig. 7. Influence of $\Delta S/D_z$ on transition of positive and negative friction along the pile

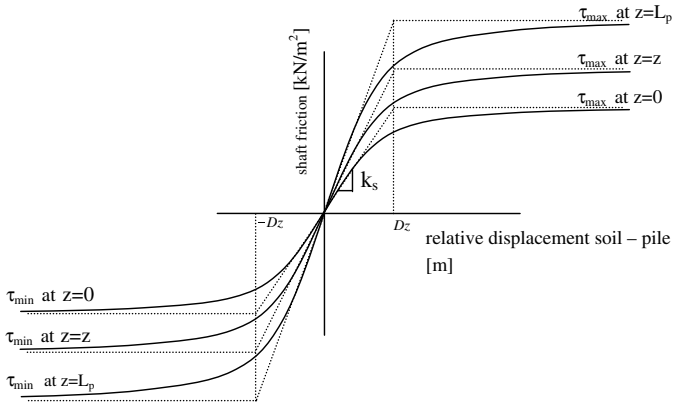

Fig. 8. Shaft friction versus relative displacement between pile and soil, maximum increasing with depth with constant D_z

negative shaft friction. The relative displacement between soil and pile at failure (D_z) is an important characteristic that determines the length of the transition zone between positive and negative shaft friction (Fig. 7). If D_z is small compared to the soil settlement gradient ΔS, the shaft friction changes from positive to negative in a short section of the pile. For larger values, the transition zone significantly increases in length. If the transition zone length is larger than the length of the pile, the maximum shaft friction will not be reached.

Analytical Solution for Increasing Maximum Shaft Capacity with Depth

The analytical solution of Eq. (8) can be extended for a linearly increasing $\tau_{\max}$ with depth (Fig. 8)

$$\tau'_{\max} = \frac{\tau_{\max;0} + (\tau_{\max;L_p} - \tau_{\max;0}) \cdot z'}{\bar{\tau}_{\max}} \tag{13}$$

where $\tau_{\max;0}$ = maximum shaft friction at $z = 0$; $\tau_{\max;L_p}$ = maximum shaft friction at $z = L_p$; and D_z = assumed to be constant for the different depths.

Combining Eq. (12) with Eq. (13) leads to

$$\frac{W\bar{\tau}_{\max}}{Q_{\max}} = \int_0^1 \tanh(S' - p'_i) \cdot [\tau_{\max;0} + (\tau_{\max;L_p} - \tau_{\max;0}) \cdot z']dz' \tag{14}$$

For the initial condition with $S_{z1} = 0$, this leads to the same solution of p'_{i1} as for the constant shaft friction with depth, as shown in Eq. (10). Eq. (11) should now include the shaft friction function with depth with the following loading and unloading branches:

$$\text{if } (S' - p'_{i2}) > -p'_{i1}$$
$$\tau' = \tanh\left(\frac{\Delta S}{D_z} \cdot z' - p'_{i2}\right) \cdot \frac{[\tau_{\max;0} + (\tau_{\max;Lp} - \tau_{\max;0}) \cdot z']}{\bar{\tau}_{\max}}$$

$$\text{if } x_1 < (S' - p'_{i2}) < -p'_{i1} \qquad \tau' = \frac{\Delta S}{D_z} \cdot z' - p'_{i2} - x'_1$$
$$\text{with } x'_1 = -\tau'_1 - p'_{i1} \quad \text{with } x'_1 \geq 0$$

$$\text{if } (S' - p'_{i2}) < x'_1$$
$$\tau' = \tanh\left(\frac{\Delta S}{D_z} \cdot z' - p'_{i2} - x'_1\right) \cdot \frac{[\tau_{\max;0} + (\tau_{\max;L_p} - \tau_{\max;0}) \cdot z']}{\bar{\tau}_{\max}}$$

To obtain the pile deformation p_i Eq. (12) can be used after solving p'_{i2} from the aforementioned branches.

For a linearly increasing maximum shaft friction with depth, the pile deformation problem includes the following dimensionless parameters: z/L_p; $W/Q_{\max}$; $\Delta S/D_z$; and $\tau_{\max;L_p}/\tau_{\max;0}$. The result for different variations of these parameters is shown in Fig. 9.

For increasing maximum shaft friction with depth, the interaction level at low initial loads (small $W/Q_{\max}$ indicating large factor of safety) is found deeper along the pile. This leads, for excavations, to a smaller pile deformation compared with the situation with constant shaft friction.

Effect of Pile Base Capacity

If the pile has base capacity, any pile deformation will also increase the base resistance (until the maximum is reached). The effect this has on the relative pile deformation compared to the soil displacement is shown in Fig. 10. Two additional dimensionless parameters are involved to take the effect of pile base capacity into account. First, this is the portion of bearing capacity found at the base compared with the total bearing capacity; $Q_b/Q_{\max}$. The graphs are for piles with 2, 20, 50, 80, and 99% end bearing, respectively. The second dimensionless characteristic is the relative displacement necessary to obtain full base capacity versus full shaft friction. In the following examples, the relative displacement to obtain full base capacity is assumed as 5% of the pile diameter and has not been varied in the graphs.

For the hypothetical option of a completely end-bearing pile, the interaction level z_p/L_p is found at the pile base ($z_p/L_p = 1$) until the pile fails. For piles with a mix of shaft friction and end bearing, the interaction level increases from 0.5 to 1.0 for low-working loads toward 0 for high-working loads. For piles that rely on base capacity for more than 50% and have a safety factor of more than 2 ($W/Q_{\max} < 0.5$), the pile deformation follows the soil at a level close to the base. Piles with larger percentages of shaft capacity or smaller safety factors settle significantly more, ultimately leading to the maximum pile deformation being equal to the maximum soil settlement, which for excavations is found at the surface.

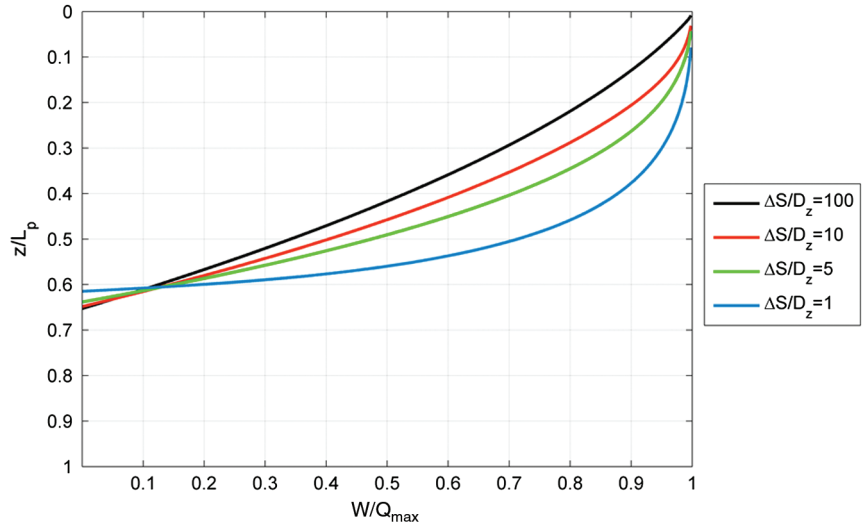

Fig. 9. (Color) Interaction factor z_p/L_p for friction piles as a function of the initial pile load $W/Q_{\max}$ for different values of $\Delta S/D_z$ and increasing maximum shaft friction with depth $\tau_{\max;L_p}/\tau_{\max;0} = 5$

Effect of Pile Flexibility

In previous sections, the analytical solutions presented have assumed infinite pile stiffness. In reality, piles, and certainly old timber piles, are not infinitely stiff.

The effect of the pile stiffness results in a nonconstant shaft friction development along the pile. The relative soil displacement $(S_z - p_i)$ changes as now not only S_z changes with depth but also p_i. This effect cannot be evaluated by dimensionless analysis because of limitations of the analytical solution. Therefore, a numerical solution is used according to Bijnagte and Luger (2000) with all other assumptions similar to the ones in section "Analytical Solution for Increasing Maximum Shaft Capacity with Depth." Fig. 11 shows the comparison between infinite and realistic pile stiffness for an increasing maximum shaft friction. For timber piles, a realistic pile stiffness E of 1×10^7 kN/m^2 is used. The effect of the pile stiffness is small for timber piles that are 10 m long and somewhat more significant for piles that are 20 m long. This indicates that for timber piles (which are commonly beneath historic buildings in Amsterdam), the effect of pile flexibility is present but small. Concrete and steel piles are stiffer, so it is expected that the effect of pile stiffness is even smaller for those piles.

Further extensions of the model are implemented in the cap module from D-Pile Group, which also includes multilayered soils, variable pile diameters, irregular soil displacement profiles, and shaft friction with depth. The basic assumptions, however, are similar to those presented in this paper. Cap interaction can also be taken into account for pile groups, but interactions between piles through the soil are not taken into account. To determine the lateral response of piles to excavations, the cap (layered) soil interaction model of D-Pile Group or FEM may be used.

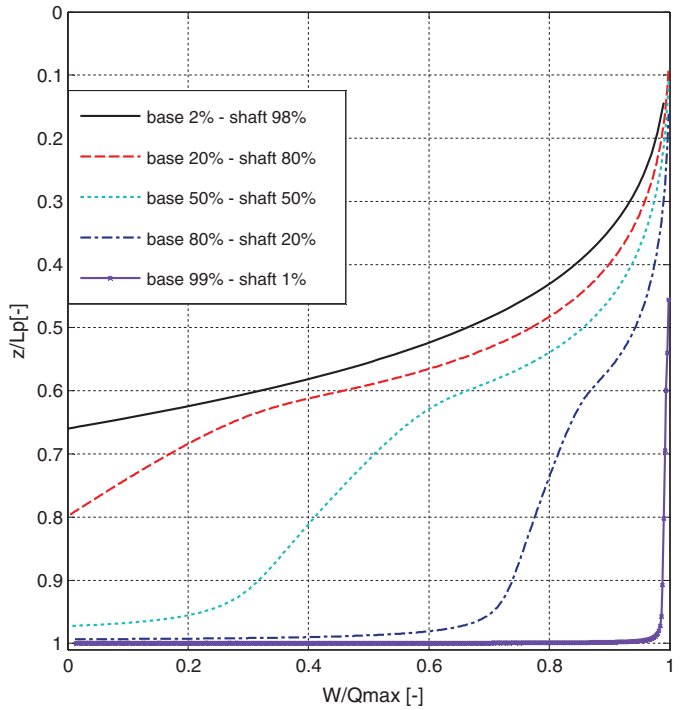

Fig. 10. (Color) Results of z_p/L_p versus $W/Q_{\max}$ for piles with 2–99% end bearing, assuming infinite pile stiffness, $\tau_{\max;L_p}/\tau_{\max;0} = 5$, and $\Delta S/D_z = 2$

Lateral Pile Response

Lateral pile response to horizontal soil deformations can be determined by FEM analysis or more simplified methods based on $p - y$ curves. For piles subjected to lateral loads from deep excavations, the green field soil displacements are determined first in an uncoupled approach. The springs are next subjected to these displacements, which determine the response of the piles. In this paper, the $p - y$ curves from API (1984) have been used for sand and clay, which both are nonlinear. The springs are not coupled, so no transfer of load takes place between the springs. In this model, the piles are connected to the pile cap, but there is no pile-soil-pile interaction. The soil resistance for each pile is considered according to API (1984) for static loads. The API continuous $p - y$ curve is approximated by five parallel elastoplastic springs (Bijnagte and Luger 2000).

The combination of axial and lateral displacements is in reality more complex than can be modeled by noncoupled springs because a combination of loading in several directions will lead to soil failure at a lower stress level than for each direction separately and also pile group effects need to be considered for a more advanced

J. Geotech. Geoenviron. Eng., 2016, 142(8): 04016034

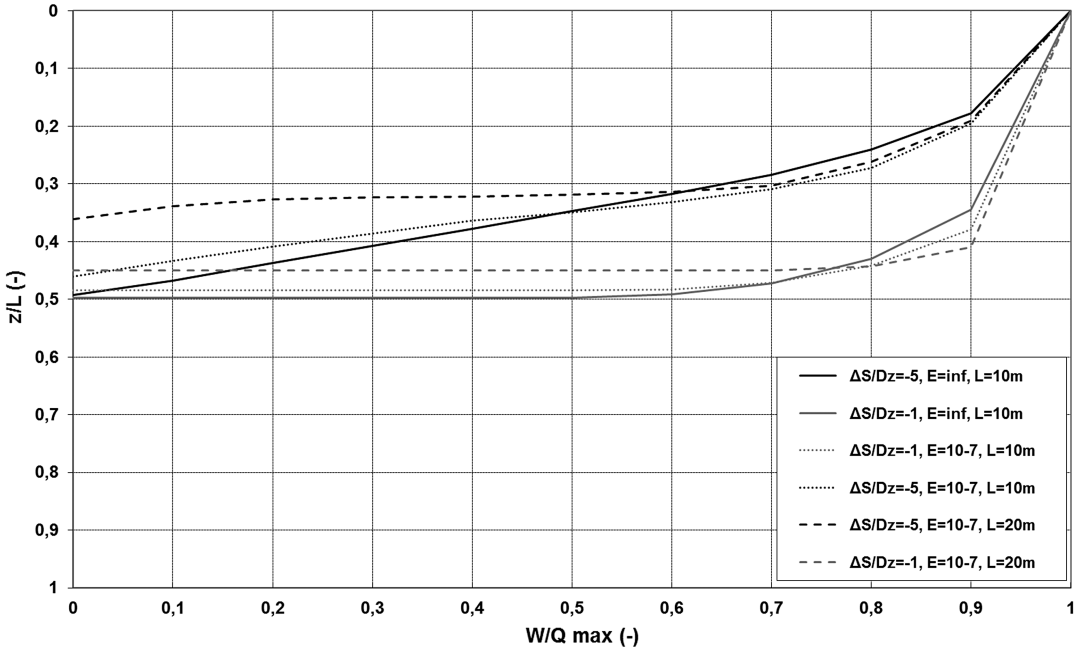

Fig. 11. Results of z_p/L_p versus $W/Q_{\max}$ with infinite and realistic stiffness for timber piles (10 m long and 20 m long, diameter $D = 0.2$ m)

approach. Both can be modeled using FEM. In many cases, however, the different loadings are considered consecutive. The D-Pile Group cap model does allow for interaction between the piles through the pile cap, as is shown in the comparison with field data presented in the following section.

Comparison with Field Data

Field data from the construction of the 9.5-km-long North South Metro line under construction in Amsterdam are compared with the model results. The project consists of two bored tunnels with three large cut and cover stations in the historic center of the Dutch capital. The stations are built to a maximum depth of approximately 33–30 m below surface level. A detailed description of the construction works is given in Korff (2013). Historic buildings found on timber piles are present at close distance from the excavations. Some of the oldest buildings (before 1925) typically are built with masonry walls, wooden floors, and a pairs of timber piles, founded approximately 12 m deep in a sand layer overlain by Holocene soft clay and peat deposits (Fig. 12).

Most of the piles under the buildings along the North South Line are approximately 100-year-old timber piles. On the basis of several pile load tests in the historic centre, it is known that the timber pile foundations have low factors of safety because of subsequent raising of the street level over the last 100 years, which caused negative skin friction to develop. Usually, some positive skin friction has developed above the pile tip to balance the negative skin friction. To obtain realistic values for the shaft friction behavior of the piles, the results of pile load tests on tapered timber piles (the diameter is 220 mm at the top and 130 mm at the tip; in calculations, an average D of 180 mm is used) were analyzed in more detail to obtain separate shaft friction curves for the soft layers and the foundation layer. The resulting curves are shown in Fig. 13.

In the Holocene clay, the maximum shaft friction develops at approximately 25 mm and in sand at approximately 15 mm of relative displacement, which is derived from tests by Hoekstra and Bokhoven (1974). This gives D_z values of 5.5 and 4 mm, respectively. In the calculations hereafter, the derived nonlinear curves of Fig. 13 have been used directly. The corresponding $\tau_{\max}$ is 5.3 and 35 kN/m^2, respectively, and the pile's Youngs' modulus is set to 8×10^6 kN/m^2. The maximum base capacity for piles with a diameter of 130 mm is reached at approximately 10% of the diameter, as can be found in common design methods. The old piles find in failure 60% of their capacity at the base, 10% as friction in the sand layer, and 30% as friction in the Holocene layers.

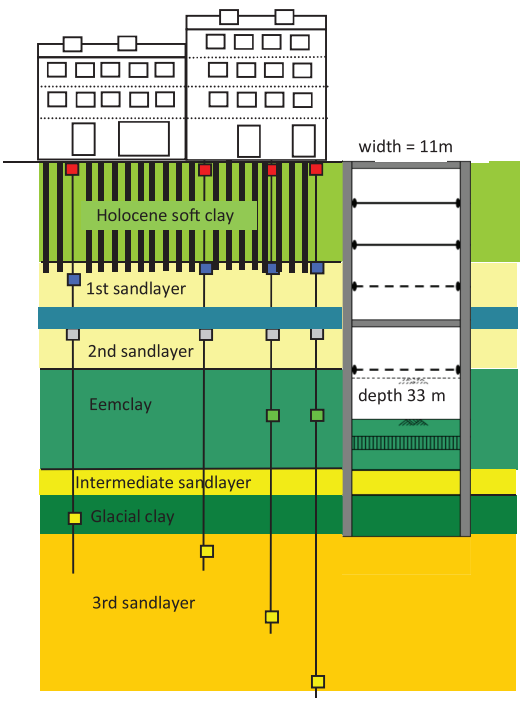

Fig. 12. (Color) Cross section of Ceintuurbaan Station with soil profile and extensometer locations

J. Geotech. Geoenviron. Eng., 2016, 142(8): 04016034

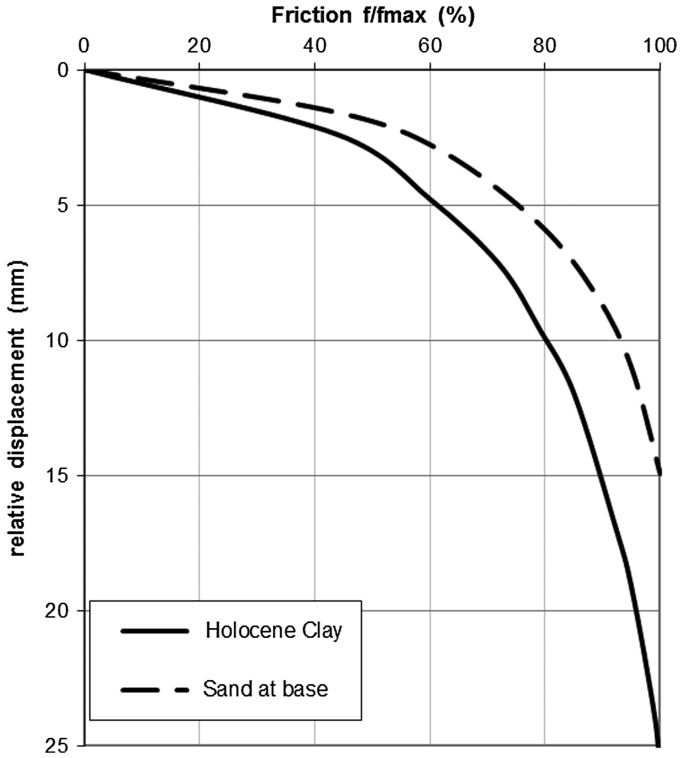

Fig. 13. Shaft friction for Holocene clay and foundation layer according to tests by Hoekstra and Bokhoven (1974) for tapered timber piles with a diameter of 220–130 mm

The measured ground settlements caused by the excavation are presented in Fig. 14, showing that the surface settlements (approximately 10 mm, in green) are larger than at the level of the base of the piles [Nieuw Amsterdams Peil (NAP)-12 m, in blue]. The settlements at deeper levels are even smaller. The settlement also decreases with the distance to the excavation, reducing to negligible values at approximately 2–2.5 times the excavated depth.

The excavation-induced settlements influenced the buildings along the length of the deep excavation and were used to analyze the soil-pile interaction at Ceintuurbaan Station. Buildings were selected according to the availability and the quality of the monitoring and historical data of the structure. Fig. 15 shows a top view of Ceintuurbaan Station with the locations of the buildings and the monitoring instruments. Fig. 16 shows the measurement points

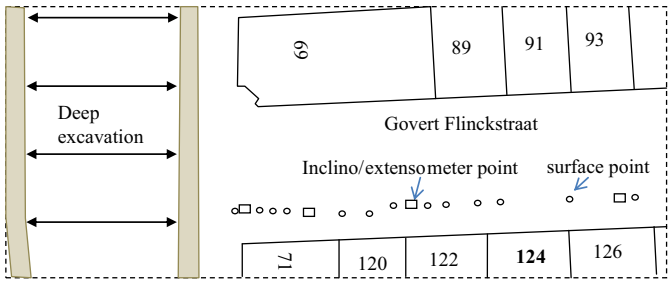

Fig. 15. Top view of deep excavation and buildings Govert Flinckstraat (Ceintuurbaan)

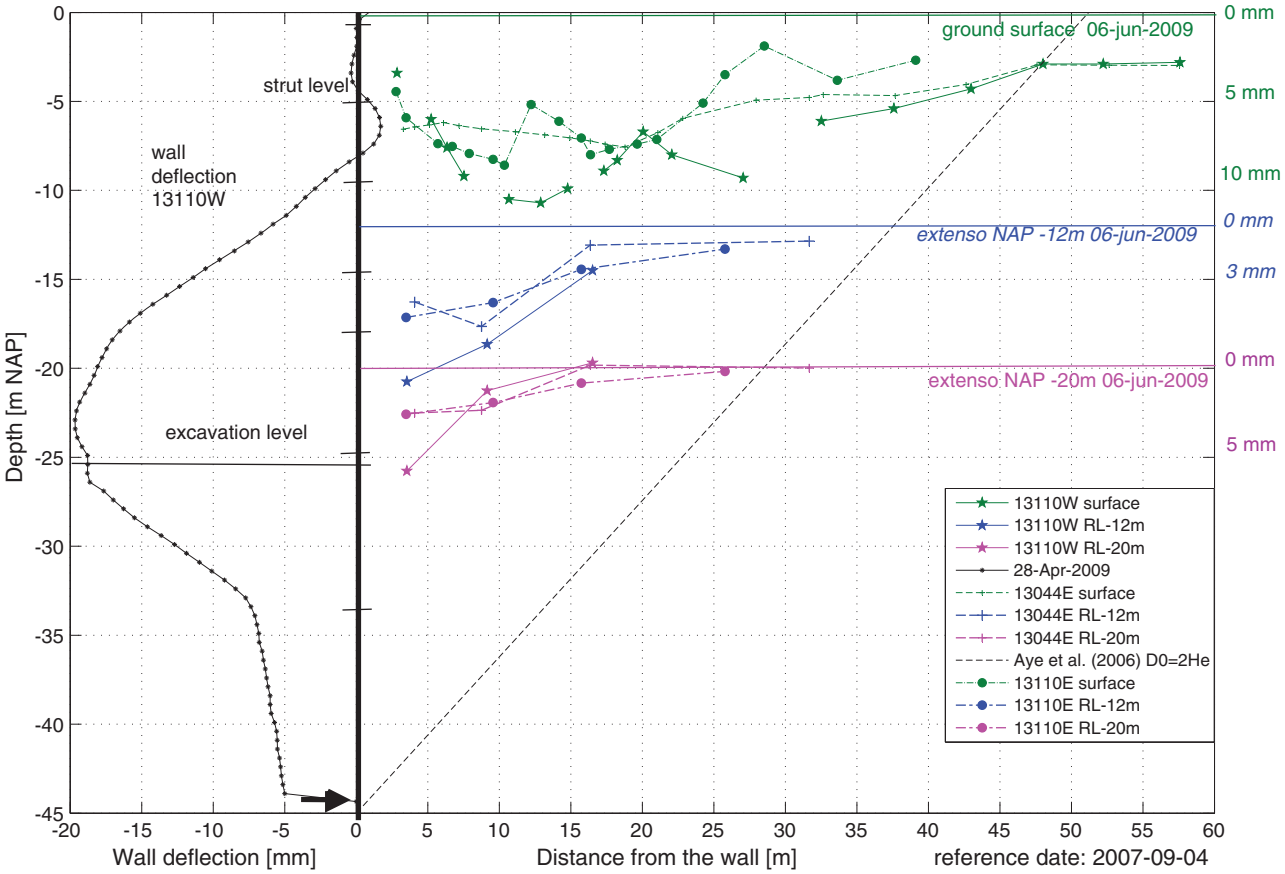

Fig. 14. (Color) Soil displacements with depth for Ceintuurbaan Station (reprinted from Korff et al. 2013)

along the façade of Govert Flinckstraat 124. The piles are located under the walls and façade of the building.

On the basis of the soil and building displacements presented in Fig. 17, the average interaction level z/L is determined in Table 1. The resulting z/L for these buildings is 0.3–0.5. When $z/L = 0$, the pile settlement is equal to the surface settlement. For z/L values between 0 and 1, a linear soil settlement profile between the surface settlement and the settlement at the sand layer (foundation level, depth L) is assumed.

With the generally available information and some typical values for Amsterdam conditions, an estimate is made for the building's initial interaction level based on the pile load and pile capacity. At Govert Flinckstraat 124, a typical Amsterdam timber pile foundation is present, and the pile load and capacity can be estimated. The 5.9-m-wide building has two piles beneath each wall section and 1.1 m between the piles along the wall. The average line working load along the wall is determined at 200 kN/m^2 for a building with floor floors, height of 12 m, width of 6 m, wall thickness of 0.22 m, a live load, and a roof load. The resulting working load per pile is

$$200/2 \times 1.1 = 110 \text{ kN}$$

The pile capacity in failure is estimated to be approximately 170 kN/pile based on the characteristics of the Dapperbuurt piles Hoekstra and Bokhoven (1974). The W/Q_{max} thus becomes 65%, leading with Fig. 18 to $z/L = 0.55$, which is slightly higher than the measured values in Table 1 for Govert Flinckstraat 124. If the pile load is somewhat higher at 120–125 kN, $W/Q_{max} = 70$–75%, and z/L fits the value taken from the measurements best.

Fig. 16. (Color) Façade with monitoring points for Govert Flinckstraat 124 (Ceintuurbaan) (reproduced by permission of Frank Kaalberg, Witteveen+Bos)

Table 1. Measured Vertical Building and Ground Displacements in the Period between June/July 2001 and June 2009 for Govert Flinckstraat 120-126 (Ceintuurbaan) and Corresponding Interaction Level z/L

Name	Building settlement (mm)	Surface settlement (mm)	Extensometer first sand layer (mm)	ΔS (mm)	Interaction level measured z/L (−)	Interaction level model z/L (−)
120B	−35.18	−46.7	−9.4	37.3	0.31	—
120A	−30.16	−46.5	−5.2	41.3	0.40	—
122B	−29.87	−51.7	−3.3	48.4	0.45	—
122A	−24.26	−49.6	−2.4	47.2	0.54	—
124B	−23.95	−44.4	−2.1	42.3	0.48	0.55
124A	−18.53	−33.2	−1.3	31.9	0.46	0.55
126B	−18.42	−29.7	−0.9	28.8	0.39	—
126A	−18.40	−28.3	0[a]	28.3	0.35	—

[a]Extrapolated value.

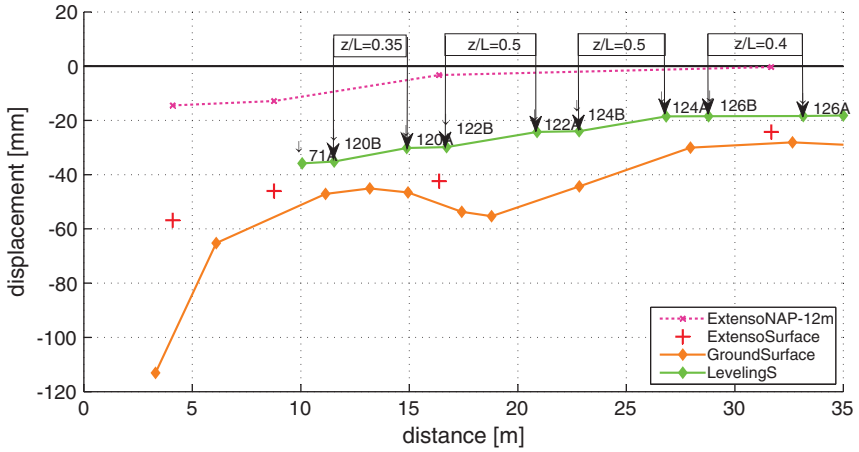

Fig. 17. (Color) Vertical ground and building displacements for Govert Flinckstraat (Ceintuurbaan, cross section 13,044 E) between June/July 2001 and June 2009, showing interaction levels (z/L) derived from measurements

J. Geotech. Geoenviron. Eng., 2016, 142(8): 04016034

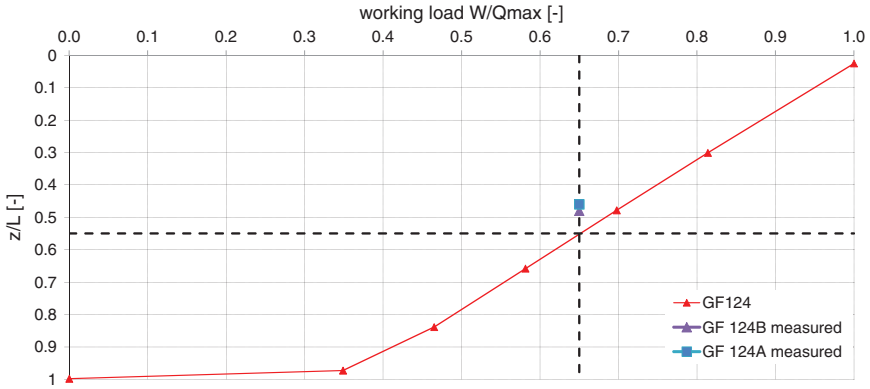

Fig. 18. (Color) Typical z/L values based on D-Pile Group calculation for pile at Ceintuurbaan with initial negative and positive skin friction fully developed because of subsidence

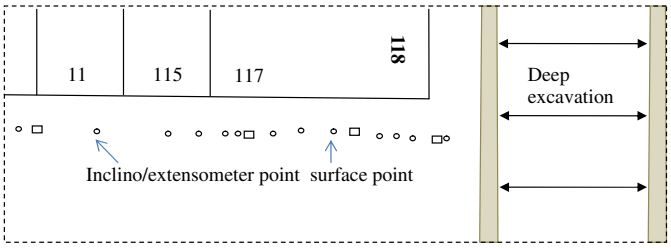

Fig. 19. Top view of deep excavation and buildings for Ferdinand Bolstraat 118 (Ceintuurbaan)

In cross section 13110WN, Ferdinand Bolstraat 118 is analyzed. The foundation of this building has been renewed by placing additional steel piles. The location of the buildings and monitoring data and the deep excavation are shown in Fig. 19, and the corresponding displacements in Fig. 20. Ferdinand Bolstraat 118 is constructed in 1893, has four regular stories, a top floor, and no basement. The top of the original foundation is found at NAP -1 m, and the designed pile load is 65 kN (the façade is perpendicular to the station) to 80 kN (walls are shared with neighboring buildings). The new piles have the same length as the original piles (base at NAP-12 m in the first sand layer) and are placed under the walls and façades at a minimum distance of 4 m from the deep excavation wall.

The building settlements in the period 2001–2009 are shown in Fig. 20, and the combined ground and building settlements with corresponding interaction level z/L in Table 2. The observed average z/L value is between 0.8 and 1.0 for this building. This is consistent with what is expected for a new, end-bearing foundation. According to Fig. 18, $z/L = 0.9$ for $W/Q_{\max} = 0.4$, which is representative for a new foundation with an overall safety factor of 2.5.

For the two buildings described, the axial interaction between soil and pile has been determined in detail according to an estimate of the foundation capacity and working load of the piles. For these buildings, the calculated interaction level z/L is in good agreement with the measured values. In most cases in practice, no detailed information is present about the foundation, but it would be practical to estimate the amount of interaction according to generally known building characteristics. For a large number of buildings along the three stations, the interaction level has been determined on the basis of the monitoring data and compared with known building characteristics. The main factor of influence appeared to be the working load $W/Q_{\max}$ because this factor determines the initial neutral level and the interaction level z/L during excavation works. The old timber pile foundations in Amsterdam generally have interaction levels z/L of approximately 0.5 for the original

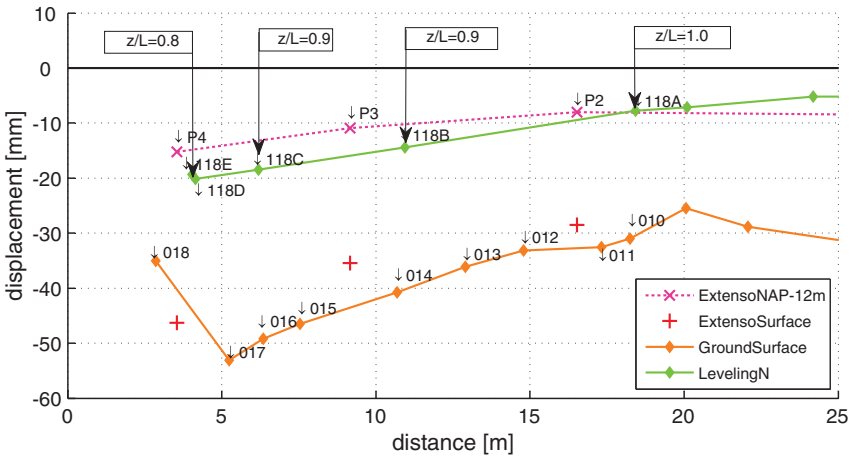

Fig. 20. (Color) Ground and building displacements for Ferdinand Bolstraat 118 (Ceintuurbaan) with distance from the deep excavation, showing interaction levels (z/L) derived from measurements

J. Geotech. Geoenviron. Eng., 2016, 142(8): 04016034

foundations and 0.8–1.0 for the renewed foundations. Modern pile foundations have interaction levels z/L of close to 1.0. This indicates that the building deformation will be close to the free-field displacement of the foundation layer (p_b).

The lateral deformations are assumed from Fig. 14 and show a maximum displacement of about 8 mm at the level of the pile tip and almost zero deflection at the top of the wall. The detailed shape over the depth of the pile is shown in Fig. 21. The lateral interaction with the soil is considered separately from the axial response, by using the nonlinear spring model of D-Pile Group with $p-y$ curves from API (1984). The springs used are presented in Fig. 22; for clay, there was an increasing stiffness with depth for the upper 4 m along the pile and constant thereafter. By assuming a maximum bending stress of 9 N/mm^2, the maximum allowable moment is 8 kNm for the piles. The soil displacements from Fig. 14 are imposed upon the $p-y$ springs. If the maximum possible soil displacement (equal to the wall deflection) is transferred to the pile closest to the excavation (which is a very conservative upper limit for piles more than 10 m away from the wall), this will cause bending moments in the pile in the order of 1.6 kN · m (Fig. 21). For an upper limit of the pile stiffness (five times the original value) or five times the increase of the soil deformation, the maximum moment is

Table 2. Building and Ground Displacements in Period between July 7, 2001, and June 24, 2009, for Ferdinand Bolstraat 118 (Ceintuurbaan) and Corresponding z/L Values

Name	Building settlement (mm)	Surface settlement (mm)	Extensometer first sand layer (mm)	z/L (−)
118A	−7.8	−30.4	−8.1	1.01
118B	−14.4	−40.2	−10.2	0.9
118C	−18.5	−49.8	−13.2	0.9
118D	−19.4	−43.6	−14.9	0.8
118E	−20.2	−43.6	−14.8	0.8

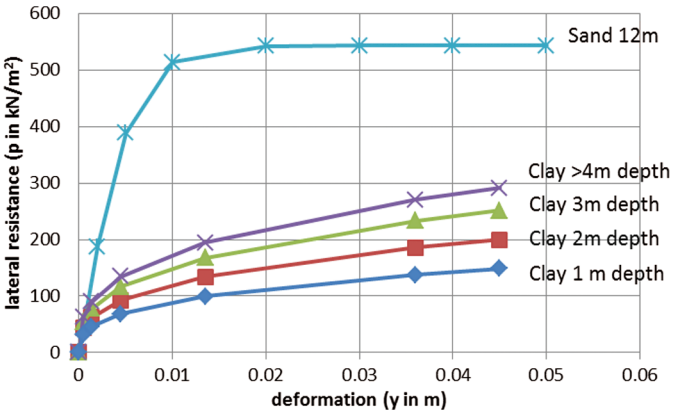

Fig. 22. (Color) p-y curves at different depths for clay and sand for pile diameter of 0.18 m according to API (1984) as used in Bijnagte and Luger (2000) (determined for a 11.5-m-thick saturated clay with c_u = 30 kN/m^2; $\gamma' = 16$ kN/m^3; empirical constant $J = 0.25$; and ϵ_{50} = 0.01 and 0.5 m sand with $\varphi' = 30°$; $\gamma' = 19.8$ kN/m^3; $K_0 = 0.5$; factor for static loads $A = 0.9$; initial modulus of subgrade reaction k = 8,145 kN/m^3; and q_c = 13.5 MPa)

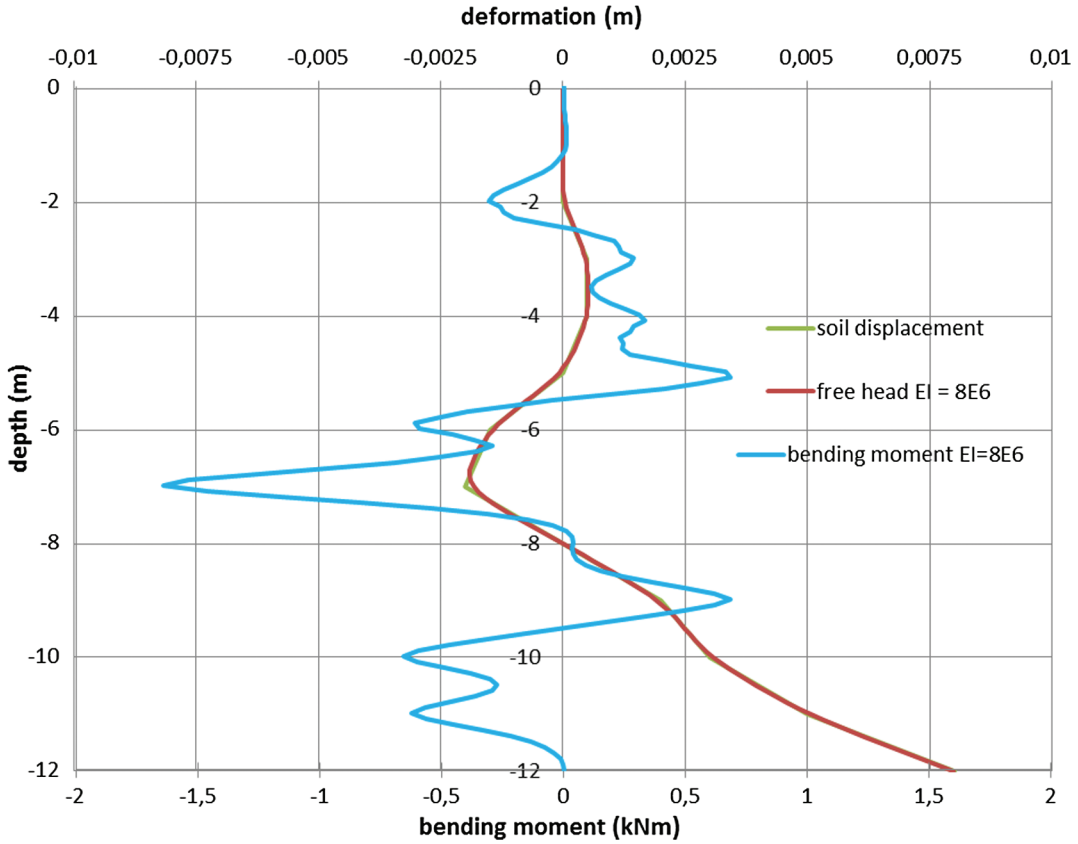

Fig. 21. (Color) Lateral displacements and bending moments in the piles at Ceintuurbaan Station calculated with D-Pile Group; the greenfield soil displacement (in green) is behind the pile deflection (in red) because the pile is very flexible and closely follows the soil displacement

still acceptable for the measured wall deflection shape. For group effects, a row of six piles is considered, spaced 1.2 m and with free-head conditions. The lateral displacement is assumed to decrease linearly between the first pile (100%) and the sixth pile (0%). The introduced moment is 2.4 kN · m, which is still acceptable. From this it is concluded that for the relatively short (compared with the excavation), very flexible old timber piles, the lateral response is not governing. For longer or stiffer piles or substantially larger soil displacements, the bending moments could become more significant.

Conclusions

The axial deformation of a pile head induced by deep excavations is determined by the sum of effects described in this paper. The pile-soil interaction contribution p_i is different for end-bearing and friction piles and can be assessed on the basis of the soil displacement at the interaction level (not to be confused with the neutral level). This interaction level z/L depends on the following dimensionless factors:

$$\frac{W}{Q_{\max}}, \quad \frac{\Delta S}{D_z}, \quad \frac{\tau_{\max;L_p}}{\tau_{\max;0}}, \quad \frac{Q_b}{Q_{\max}}, \quad \text{and} \quad \frac{D}{D_z}$$

Common generalizations that end-bearing piles settle with the soil at the base level, and friction piles with the surface level are valid only for certain idealized cases and typically represent lower and upper bounds for the actual pile settlement. The actual pile settlement is found in between those values on the basis of the following conditions:

- The interaction level is found at the base of the pile if the contribution of the shaft friction to the total bearing capacity is less than 50% and the factor of safety is at least 2 ($W/Q_{\max} < 0.5$);
- Piles with larger percentages of shaft friction or smaller safety factors settle significantly more. A good first estimate for such piles would be to assume the interaction level to be halfway down the pile; and
- For extreme cases of $W/Q_{\max}$, the maximum pile settlement will become equal to the maximum soil settlement, which for deep excavations is normally found at the ground surface.

The measurements during construction activities for the deep excavations of the North South Line project in Amsterdam presented in this paper show an interaction level z/L of 0.3–0.8 (average of 0.5) for most original timber pile foundations and 0.8–1.0 for most renewed foundations. For buildings for which the pile load and capacity can be estimated, the analytical model shows a good correlation with the calculated interaction factor z/L. The measured lateral ground deflections over the length of the 12-m-long piles were small (maximum of 8 mm) and in this case would have caused only minor bending moments in the piles. For longer or stiffer piles or substantially larger soil displacements, the bending moments could become more significant.

The axial interaction model and dimensionless graphs are suitable to show the distinction between friction and end-bearing piles and the influence of the working load and the factor of safety. They can best be used as a preliminary assessment and for a more detailed understanding of the mechanisms. The spring models presented are best suitable in case of layered soil, tapered piles, and significant pile flexibility and are necessary to determine lateral deflections. To further develop the understanding of the pile-soil interaction, there is a clear need for more fully instrumented (subsoil, pile, and building) case studies (either in the field or on a model scale) and advanced calculation models to study the combined effect of axial and lateral response of piles close to deep excavations.

Acknowledgments

This paper is based on the first author's Ph.D. study at Cambridge University in cooperation with the Netherlands Centre of Underground Construction.

Notation

The following symbols are used in this paper:

A = cross-sectional area of pile;
D = pile diameter;
D_z = relative displacement between soil and pile at failure;
k_s = initial stiffness;
L_p = length of the pile;
p = axial deformation of the pile head;
p_b = pile settlement caused by soil displacement below the base of the pile;
p_i = pile settlement related to the development of negative (and/or positive) skin friction;
p_r = pile settlement caused by redistribution of pile load;
p_s = pile settlement caused by lower stress levels;
$Q_{\max}$ = maximum bearing capacity of the pile;
Q_b = pile base capacity;
q_b = average foundation pressure around the pile base;
S_0 = soil displacement at $z = 0$;
S_{lp} = soil displacement at $z = L_p$;
S_z = displacement of the soil at depth z;
W = working load on the pile;
z = depth;
ΔS = soil settlement gradient;
τ = shaft friction along the pile;
$\tau_{av;\max}$ = average shaft friction over the pile length;
$\tau_{\max}$ = maximum shaft friction;
$\tau_{\max;0}$ = maximum shaft friction at $z = 0$; and
$\tau_{\max;L_p}$ = maximum shaft friction at $z = L_p$.

References

API (American Petroleum Institute). (1984). "Recommended practice for planning, designing, and constructing fixed offshore platforms." Washington, DC.

Aye, Z. Z., Karki, D., and Schulz, C. (2006). "Ground movement prediction and building damage risk-assessment for the deep excavations and tunneling works in Bangkok subsoil." *Proc., Int. Symp. on Underground Excavation and Tunnelling*, ITA, Bangkok, Thailand, 281–297.

Bezuijen, A., and Van der Schrier, J. (1994). "The Influence of a bored tunnel on pile foundations." *Proc. Centrifuge*, 94, 681–686.

Bijnagte, J. L., and Luger, H. J. (2000). "3D modelling of single piles and pile groups. Manual D-Pile Group version 5.1." Deltares, Delft, Netherlands.

Chen, L. T., Poulos, H. G., and Loganathan, N. (1999). "Pile responses caused by tunneling." *J. Geotech. Geoenviron. Eng.*, 10.1061/(ASCE)1090-0241(1999)125:3(207), 207–215.

Clough, G. W., and O'Rourke, T. D. (1990). "Construction induced movements of in-situ walls." *Design and performance of earth retaining structures*, ASCE, Reston, VA, 439–470.

Goh, A. T. C., Teh, C. I., and Wong, K. S. (1997). "Analysis of piles subjected to embankment induced lateral soil movements." *J. Geotech. Geoenviron. Eng.*, 10.1061/(ASCE)1090-0241(1997)123:9(792), 792–801.

Goh, A. T. C., Wong, K. S., The, C. I., and Wen, D. (2003). "Pile response adjacent to braced excavation." *J. Geotech. Geoenviron. Eng.*, 10.1061/(ASCE)1090-0241(2003)129:4(383), 383–386.

Hoekstra, J., and Bokhoven, W. (1974). "Systematisch funderingsonderzoek van de Dapperbuurt." Laboratorium voor Grondmechnica, Delft, Netherlands (in Dutch).

Jacobsz, S. W., Bowers, K. H., Moss, N. A., and Zanardo, G. (2005). "The effects of tunnelling on piled structures on the CTRL." *Geotechnical aspects of underground construction in soft ground, Amsterdam*, Taylor & Francis Group, London, 115–122.

Kaalberg, F. J., Teunissen, E. A. H., Van Tol, A. F., and Bosch, J. W. (2005). "Dutch research on the impact of shield tunnelling on pile foundations." *Geotechnical aspects of underground construction in soft ground*, Taylor & Francis Group, London, 123–131.

Korff, M. (2013). *Response of piled buildings to the construction of deep excavations*, IOS Press, Rotterdam, Netherlands.

Korff, M., Mair, R. J., and Van Tol, A. F. (2013). "Ground displacements related to deep excavation in Amsterdam." *Proc., 18th Int. Conf. on Soil Mechanics and Geotechnical Engineering*, Presses des Ponts, Paris, 2779–2782.

Lee, G. T. K., and Ng, C. W. W. (2005). "Three-dimensional numerical simulation of tunnelling effects on an existing pile." *Proc., 5th Int. Symp. on Geotechncial Aspects of Underground Construction in Soft Ground*, K. J. Bakker, A. Bezuijen, W. Broere, and E. A. Kwast, eds., A.A. Balkema, Amsterdam, Rotterdam, Netherlands, 139–144.

Leung, C. F., Chow, Y. K., and Shen, R. F. (2000). "Behavior of pile subject to excavation-induced soil movement." *J. Geotech. Geoenviron. Eng.*, 10.1061/(ASCE)1090-0241(2000)126:11(947), 947–954.

Leung, C. F., Lim, J. K., Shen, R. F., and Chow, Y. K. (2003). "Behavior of pile groups subject to excavation-induced soil movement." *J. Geotech. Geoenviron. Eng.*, 10.1061/(ASCE)1090-0241(2003)129:1(58), 58–65.

Loganathan, N., Poulos, H. G., and Xu, K. J. (2001). "Ground and pile-group responses due to tunnelling." *Soils Found.*, 41(1), 57–67.

Ong, C. W., Leung, C. F., Yong, K. Y., and Chow, Y. K. (2007). "Performance of pile due to tunneling-induced soil movements." *Proc., 33rd ITA–AITES World Tunnel Congress—Underground Space—4th Dimension of Metropolises*, Vol. 1, CRC Press, Boca Raton, FL, 619–624.

Ong, D. E. L., Leung, C. F., and Chow, Y. K. (2006). "Pile behavior due to excavation-induced soil movement in clay. I: Stable wall." *J. Geotech. Geoenviron. Eng.*, 10.1061/(ASCE)1090-0241(2006)132:1(36), 36–44.

Ong, D. E. L., Leung, C. F., and Chow, Y. K. (2009). "Behavior of pile groups subject to excavation-induced soil movement in very soft clay." *J. Geotech. Geoenviron. Eng.*, 10.1061/(ASCE)GT.1943-5606.0000095, 1462–1474.

Poulos, H. G., and Chen, L. F. (1997). "Pile response due to excavation induced lateral soil movement." *J. Geotech. Geoenviron. Eng.*, 10.1061/(ASCE)1090-0241(1997)123:2(94), 94–99.

Xu, K. J., and Poulos, H. G. (2001). "3-D elastic analysis of vertical piles subjected to 'passive' loadings." *Computers and Geotechnics*, 28(5), 349–375.

Zhang, R., Zheng, J., Pu, H., and Zhang, L. (2011). "Analysis of excavation-induced responses of loaded pile foundations considering unloading effect." *Tunnelling Underground Space Technol.*, 26(2), 320–335.